# Fatty Acid Interactions with a Helix-less Variant of Intestinal Fatty Acid-Binding Protein†

David P. Cistola,* Keehyuk Kim, Hans Rogl,‡ and Carl Frieden*

*Department of Biochemistry and Molecular Biophysics, Washington University School of Medicine, St. Louis, Missouri 63110-1093*

*Received December 11, 1995; Revised Manuscript Received March 6, 1996*⊗

ABSTRACT: Intestinal fatty acid-binding protein (I-FABP) binds a single molecule of long-chain fatty acid in an enclosed cavity surrounded by two antiparallel $\beta$-sheets. The structure also contains two short α-helices which form a cap over one end of the binding cavity adjacent to the methyl terminus of the fatty acid. In this study, we employed a helix-less variant of I-FABP known as Δ17-SG [Kim, K., Cistola, D. P., & Frieden, C. (1996) *Biochemistry 35*, 7553−7558] to investigate the role of the helical region in maintaining the integrity of the binding cavity and mediating the acquisition of ligand. Fluorescence and NMR experiments were used to characterize the energetic, structural, and kinetic properties of fatty acid binding to this variant, and the results were compared and contrasted with those of wild-type I-FABP and a single-site mutant, R106T. Remarkably, oleate bound to Δ17-SG with a dissociation constant of 4.5 $\mu$M, a value comparable to that for R106T and approximately 20−100-fold higher than that for wild-type I-FABP. Heteronuclear two-dimensional NMR spectra for [2-$^{13}$C]palmitate complexed with Δ17-SG revealed a pattern nearly identical to that observed for the wild-type protein, but distinct from that for R106T. In addition, the ionization behavior of bound [1-$^{13}$C]palmitate and the nearest neighbor patterns for [2-$^{13}$C]palmitate derived from $^{13}$C-filtered NOESY experiments were very similar for Δ17-SG and the wild-type protein. These results implied that the fatty acid−protein interactions characteristic of the carboxyl end of the fatty acid binding cavity in the wild-type protein were essentially intact in the helix-less variant. In contrast, $^{13}$C-filtered NOESY spectra of [16-$^{13}$C]palmitate bound to Δ17-SG indicated that the fatty acid−protein interactions at the methyl end of the binding cavity were disrupted. As determined by stopped-flow fluorescence, the observed ligand association rates for both Δ17-SG and wild-type I-FABP increased with increasing oleate concentration, but only the wild-type protein exhibited a limiting value of 1000 $s^{-1}$. This rate-limiting process was interpreted as a conformational change involving the helical region that allows the ligand access to the internal cavity. Simulation and fitting of the kinetic results yielded ligand association rates for Δ17-SG and wild-type I-FABP that were comparable. However, the dissociation rate for wild-type protein was 16-fold lower than that for Δ17-SG. We conclude that the α-helices of I-FABP are not required to maintain the integrity of the fatty acid binding cavity but may serve to regulate the affinity of fatty acid binding by selectively altering the dissociation rate constant. In this manner, conformational changes involving the α-helical domain may help control the transfer of fatty acids within the cell.

Intestinal fatty acid-binding protein (I-FABP)[1] belongs to a family of intracellular lipid-binding proteins that contains at least 20 members (Banaszak *et al.*, 1994; Veerkamp & Maatman, 1995). It binds a single molecule of long-chain fatty acid in an interior cavity surrounded by two five-stranded antiparallel $\beta$-sheets (Sacchettini & Gordon, 1993). The structure also contains two short α-helices, spanning residues 15−31, which form a cap over one end of the binding cavity. To address questions regarding the role of the helices in ligand entry and protein stability, we engineered a helix-less variant of I-FABP by deleting residues 15−31 and replacing them with a two-residue linker, Ser-Gly. Our initial characterization of the conformation and stability of this I-FABP variant, known as Δ17-SG, is described in the accompanying paper (Kim *et al.*, 1996). In brief, Δ17-SG folded reversibly into a fairly stable structure which had an overall $\beta$-clam conformation similar to that of the wild-type protein, except for a selective loss of α-helix content. It appeared that Δ17-SG is an essentially helix-less, all-$\beta$-sheet variant of I-FABP.

The purpose of the present study was to investigate the fatty acid-binding properties of Δ17-SG. We employed fluorescence and NMR spectroscopies in order to characterize the energetics and kinetics of binding and to probe the local environments near the methyl and carboxyl termini of the

†This work was supported by National Institutes of Health Grants DK48046 (to D.P.C.) and DK13332 (to C.F.). D.P.C. was supported by a Johnson & Johnson/Merck Research Scholar Award from the American Digestive Health Foundation.

* To whom correspondence should be addressed: Campus Box 8231, Washington University School of Medicine, 660 South Euclid Avenue, St. Louis, MO 63110. Phone: 314-362-3344 or -4382. Fax: 314-362-7183.

‡ Present address: Brandlberger Strasse 85, 93057 Regensburg, Germany.

⊗ Abstract published in *Advance ACS Abstracts,* May 15, 1996.

[1] Abbreviations: I-FABP, *Escherichia coli*-derived rat intestinal fatty acid-binding protein; Δ17-SG, a mutant form of I-FABP in which residues E15−G31 were deleted and Ser-Gly was inserted in their place; R106T, a site-specific mutant of I-FABP where Arg106 has been replaced by Thr; HSQC, two-dimensional $^{1}$H/$^{13}$C heteronuclear single quantum correlation; NOESY−HSQC, two-dimensional $^{13}$C-filtered $^{1}$H−$^{1}$H nuclear Overhauser and exchange spectroscopy.

S0006-2960(95)02912-6 CCC: $12.00 

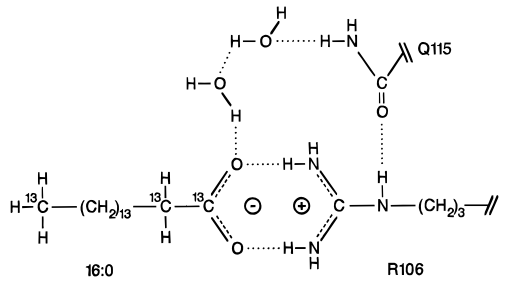


FIGURE 1: Schematic representation of ligand−protein interactions occurring at the carboxyl end of the fatty acid-binding cavity of I-FABP and the positions of $^{13}C$ enrichment used in this study. These interactions are based on evidence from X-ray crystallography (Sacchettini *et al.*, 1989) and NMR spectroscopy (Cistola *et al.*, 1989; footnote 2).

bound fatty acid. The results for Δ17-SG are compared and contrasted with those for wild-type I-FABP and the single-site mutant, R106T. In the wild-type complex, the methyl end of the fatty acid interacts with side chains in the α-helical region, whereas the carboxyl end interacts primarily with Arg106, forming an ion pair/hydrogen bond network (Figure 1). The results indicated that the interaction with Arg106 was maintained in Δ17-SG but that interactions at the methyl end of the fatty acid were disrupted. On the basis of kinetic observations, we conclude that wild-type I-FABP undergoes a conformational change that allows the ligand to enter the binding cavity and that this conformational change involves the α-helical region.

## MATERIALS AND METHODS

*Materials*. The oleic acid used for fluorescence studies was obtained from Sigma (St. Louis, MO) and dissolved in 0.1 M potassium hydroxide to prepare a 5 mM stock solution. The selectively $^{13}C$-enriched palmitic acids, 99%-[1-$^{13}C$], -[2-$^{13}C$], and -[ω-$^{13}C$], were purchased from Cambridge Isotope Labs, Inc. Their isotopic and chemical purity was established by one-dimensional $^1H$ and $^{13}C$ NMR of samples dissolved in deuteriochloroform.

*Sample Preparation*. The methods used for biosynthesis and purification of wild-type and mutant I-FABPs are detailed elsewhere (Jakoby *et al.*, 1993; Kim *et al.*, 1996). Samples containing fatty acid−protein complexes for NMR were prepared as in Cistola *et al.* (1989).

*Stopped-Flow Fluorescence Spectroscopy*. Kinetic and equilibrium measurements of oleate binding to I-FABP were performed using an Applied Photophysics stopped-flow spectrophotometer (Model SFMV12) interfaced to an Acorn Archimedes 420 computer. Changes in fluorescence ($\lambda_{excitation}$ = 290 nm; $\lambda_{emission}$ > 305 nm with an Oriel WG305 Schott glass filter) were followed at 20 °C in 20 mM sodium pyrophosphate and 0.25 mM EDTA (pH 9.0). The protein, at a concentration of 1−2 μM, was mixed with an equal volume of potassium oleate in the same buffer so that the final oleate concentrations ranged from 0.2 to 100 μM for wild-type I-FABP and 2 to 100 μM for Δ17-SG. At and below 100 μM, no self-association of oleate was observed on the basis of light scattering. Under these conditions, the dead time of the stopped-flow instrument was less than ~2 ms (Tonomura *et al.*, 1978). The data of four to five individual experiments at each set of conditions were averaged and then analyzed by exponential fitting routines. Single or double exponential equations were used to fit the equilibrium binding data. Kinetic simulation and fitting were performed using KINSIM and FITSIM software as previously described (Barshop *et al.*, 1983; Zimmerle & Frieden, 1989).

*Isothermal Titration Calorimetry*. Calorimetry experiments were performed at 25 °C using a Microcal OMEGA differential titrating calorimeter interfaced to a PC-compatible computer and analyzed using ORIGIN software (Wiseman *et al.*, 1989). Isotherms were obtained for oleate binding to R106T, but not Δ17-SG, since preliminary results for the latter exhibited enthalpy changes too small to quantitate under these conditions. Results for the wild-type protein have been reported previously (Jakoby *et al.*, 1993; Miller & Cistola, 1993). All experiments were performed in a buffer containing 20 mM potassium phosphate, 50 mM KCl, and 0.05% $NaN_3$ (pH 7.25). Thirty aliquots, 6 μL each, of the oleate solution (5 mM) were injected into the sample cell containing the protein solution (308 μM). To control for the heat associated with possible phase changes in the oleate upon injection as well as the heat of dilution, control experiments were performed by injecting the oleate solution into buffer lacking protein. The resulting heats, small in magnitude compared with the heat of binding, were subtracted from the total values obtained in the presence of protein. The corrected data were fit to a simple binding model assuming a single class of binding sites. The final dissociation constants are reported as the mean ± standard deviation for four independent experiments

*NMR Spectroscopy*. All spectra were accumulated using instrumentation and procedures described elsewhere (Hodsdon *et al.*, 1995; Kim *et al.*, 1996), except as follows. The pulse sequence used for the two-dimensional $^1H/^{13}C$ HSQC experiments was essentially the same as that shown in Figure 1c of Bax *et al.* (1990). The pulse sequence for the two-dimensional $^1H/^{13}C$ isotope-filtered NOESY experiments (NOESY−HSQC) was similar to that of Ikura *et al.* (1990) except that an HSQC subsequence was substituted for HMQC. Carbon decoupling during $^1H$ acquisition was achieved using a GARP-1 scheme (Shaka *et al.*, 1985), using a decoupling field strength of 2500 Hz centered at 42.72 ppm. In most cases, a very weak presaturation pulse (0.6−2 μW) was applied during the relaxation delay to suppress the solvent resonance. Proton-decoupled $^{13}C$ NMR experiments were perfomed as detailed elsewhere (Jakoby *et al.*, 1993). $^1H$ and $^{13}C$ chemical shifts were referenced to external sodium 3-(trimethylsilyl)propionate-2,2,3,3-$d_4$ (TSP) as in Hodsdon *et al.* (1995), except for the values reported in Figure 4, which were reported relative to external tetramethylsilane (TMS) in $CDCl_3$ ($\delta_{tms} = \delta_{tsp} - 2.72$ ppm).

## RESULTS

*Ligand Binding Affinity*. A 30% enhancement of intrinsic protein fluorescence occurs upon oleate binding to both Δ17-SG and the wild-type I-FABP. This enhancement was used to determine dissociation constants for oleate binding to both proteins as well as the association and dissociation rate

[2] The three-dimensional solution structure of I-FABP complexed with palmitate has recently been determined on the basis of 3889 distance constraints derived from three-dimensional $^{13}C$- and $^{15}N$-resolved NOESY data (M. E. Hodsdon, J. W. Ponder, and D. P. Cistola, manuscript submitted).

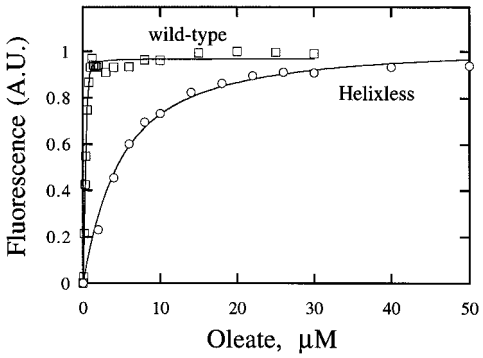


FIGURE 2: Fluorescence binding isotherms for oleate interaction with wild-type (□) and Δ17-SG (○) I-FABP at 20 °C. These equilibrium binding data were collected using a stopped-flow apparatus as described in Materials and Methods. Aliquots of the protein solution (Δ17-SG, 2.0 $\mu$M; wild-type, 1.0 $\mu$M) were mixed with an equal volume of oleate solutions (Δ17-SG, 4−100 $\mu$M; wild-type, 0.2−30 $\mu$M), and the last 5% of the stopped-flow data at each concentration were averaged, subtracted from the averaged base line value, and plotted. The data points were fit to a single-site binding model. The *y*-axis is in arbitrary units.

constants (see below). These experiments were performed at pH 9.0 since (i) the wild-type protein is stable at pH 9 and appears to bind fatty acid in a manner similar to that at pH 7.2 and (ii) the fatty acid has less tendency to self-associate under these conditions. Oleate forms a bilayer phase at pH 7 at concentrations above ~0.01 mM but at pH 9 forms a micellar phase at concentrations above ~1 mM (Cistola *et al.*, 1986, 1988; Cistola & Small, 1990). The higher monomer solubility of oleate at pH 9 was advantageous for the present fluorescence binding and kinetic studies.

Attempts to determine the dissociation constants by measuring fluorescence changes upon addition of small amounts of concentrated oleate solutions proved unreliable. In addition, the high affinity of oleate binding required the use of rather low protein concentrations, and apparent binding to the walls of the cuvette gave nonreproducible results. Instead, these equilibrium experiments were performed in a stopped-flow apparatus since only a 2-fold dilution of the oleate stock solution was required. Oleate solutions were rapidly mixed with protein, and the final equilibrium fluorescence emission intensities at wavelengths >305 nm were monitored as a function of ligand concentration. Prewashing of the ligand syringes of the stopped-flow apparatus was used to circumvent the surface binding problem.

The equilibrium binding data for Δ17-SG are displayed in Figure 2. The data, fit to a single-site binding model and yielded a dissociation constant of 4.5 ± 0.5 $\mu$M. In addition, $K_d$ values were calculated from the ratio of the off and on rates determined from kinetic simulation and fitting of the stopped-flow experiments. As shown in Table 1, the $K_d$ values for oleate binding to Δ17-SG determined by either method were similar, ~4−5 $\mu$M. These values were approximately 20−100-fold higher than those measured for wild-type I-FABP. The $K_d$ value for oleate binding to R106T, as determined by isothermal titration calorimetry, was ~1 $\mu$M.

*Ligand Binding Location.* Two-dimensional $^1$H/$^{13}$C HSQC NMR experiments were employed in order to probe the structural and dynamical features of fatty acid−protein interactions. Figure 3 exhibits spectra for 1:1 complexes

Table 1: Dissociation Constants for Oleate Binding to Wild-Type and Mutant Variants of I-FABP

| | $K_d$ ($\mu$M) | |
|---|---|---|
| I-FABP type | from equilibrium analysis | from kinetic analysis[a] |
| Δ17-SG | 4.5 ± 0.5[b] | 4.0 ± 0.2[b] |
| wild-type | 0.042 ± 0.010[b] | 0.21 ± 0.02[b] |
| | 0.28 ± 0.01[c] | |
| | 0.039 ± 0.009[d] | |
| | 0.2 ± 0.1[e] | |
| R106T | 1.1 ± 0.2[f] | |

[a] Calculated from the kinetic simulations (Table 2) using the following equations: $K_d = k_{-2}(k_1 + k_{-1})/k_1k_2$ (Scheme 1) for wild-type or $K_d = k_{-2}/k_2$ (Scheme 2) for Δ17-SG. [b] This study. Determined by stopped-flow fluorescence; pH 9.0, 20 °C, 20 mM sodium pyrophosphate, and 0.25 mM EDTA. [c] Richieri *et al.* (1992). Determined by fluorescence using acrylodan-derivatized I-FABP; pH 7.4, 37 °C, 10 mM HEPES, 150 mM NaCl, 5 mM KCl, and 1 mM $NaHPO_4$. [d] Richieri *et al.* (1994). Determined by fluorescence using unmodified I-FABP; same sample conditions as in footnote c. [e] Jakoby *et al.* (1993). Determined by isothermal titration calorimetry; pH 7.2, 25 °C, 20 mM $KHPO_4$, 50 mM KCl, and 0.05% $NaN_3$. [f] This study; same conditions as in footnote e.

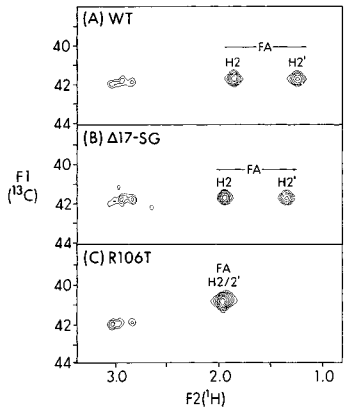


FIGURE 3: Two-dimensional $^1$H/$^{13}$C HSQC spectra for [2-$^{13}$C]-palmitate complexed with wild-type (A), Δ17-SG (B), and R106T (C) I-FABP at 25 °C. The protein concentrations were 2.0, 1.3, and 2.0 mM, respectively. The less intense peaks at $^1$H ≈ 3 ppm represent natural abundance methylene resonances for Asn, Lys, and Arg residues (Hodsdon *et al.*, 1995): number of transients, 32; number of complex points (F2), 1024 zero-filled to 2048; spectral width (F2), 6500 Hz; number of complex points (F1), 400 zero-filled to 1024; and spectral width (F1), 10 000 Hz. The spectra were processed with Gaussian apodization in both dimensions.

between [2-$^{13}$C]-16:0 and three different forms of I-FABP. The labeled peaks represent through-bond correlations between the 2-methylene carbon (*y*-axis) and protons (*x*-axis) of the bound fatty acid. The spectrum for the wild-type protein (Figure 3A) exhibited two well-separated resonances for the 2-methylene protons of the single bound fatty acid. Thus, the local microenvironments of the H2 and H2′ protons are distinct and are not averaged by possible internal motions of the bound fatty acid on the chemical shift time scale of ~3 ms. This result is consistent with independent observations that the carboxyl end of the bound fatty acid is rigidly held in a hydrogen-bonding network (Figure 1). In contrast, disruption of this hydrogen-bonding network by site-specific mutation of R106 to T results in a coalescence of the two methylene proton resonances into a single averaged resonance (Figure 3C). Essentially identical spectra have been obtained for R106Q, R106A, and R106E (not shown). However, the Δ17-SG variant (Figure 3B) exhibited a spectral signature very similar to that for the wild-type

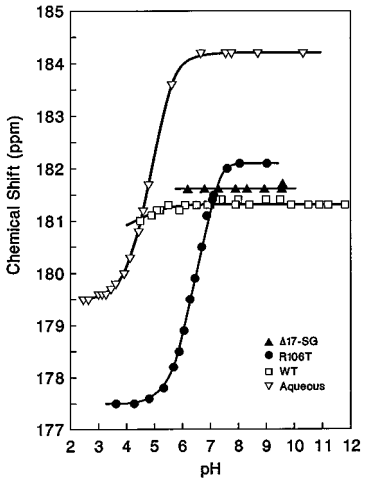


FIGURE 4: $^{13}$C NMR ionization curves for [1-$^{13}$C]palmitate bound to Δ17-SG (filled triangles) and R106T (filled circles) at 25 °C. Also shown are data for wild-type I-FABP (squares) and monomeric octanoic acid in the absence of protein (inverted triangles), taken from Cistola *et al.* (1989, 1987), respectively. The protein concentrations for Δ17-SG and R106T were 0.7 and 1.9 mM, respectively. The experiments were performed and analyzed as in Jakoby *et al.* (1993).

protein, implying that the hydrogen-bonding interaction between the fatty acid and protein was intact.

To further assess the interactions between the carboxyl end of the fatty acid and the protein, ionization curves were generated by measuring the chemical shift values for the carboxyl carbon of the bound fatty acid as a function of pH (Figure 4). The curve for wild-type protein (Figure 4, open squares) showed little ionization of the fatty acid carboxyl group over a wide pH range, consistent with an apparent p$K_a$ value < 4 and the participation of the carboxyl group in an ion pair interaction with the protein [Figure 1 and Cistola *et al.* (1989)]. Fatty acid bound to Δ17-SG (filled triangles) exhibited a similar profile with no detectable ionization between pH 5.8 and 9.6.[3] In contrast, fatty acid bound to R106T (filled circles) exhibited a full ionization profile similar to that for monomeric fatty acid in aqueous solution (inverted triangles). The apparent p$K_a$ for fatty acid bound to R106T was 6.4 ± 0.1, as compared to 4.8 ± 0.1 for monomeric fatty acid in aqueous solution (Cistola *et al.*, 1987). The elevated p$K_a$ for fatty acid bound to R106T was indicative of the absence of a fatty acid−protein ion pair interaction and the presence of a low dielectric environment inside the binding cavity.

Through-space interactions (<5 Å) between the carboxyl end of the fatty acid and the protein were probed using $^{13}$C-filtered NOESY−HSQC experiments and 2-$^{13}$C-enriched palmitate. As shown in Figure 5, NOESY cross-peaks corresponding to through-space correlations between the fatty acid methylene protons and aromatic and aliphatic side chain protons were observed. For the wild-type protein, these protein resonances have been assigned (Hodson *et al.*, 1995; footnote 2). Though not superimposable, the NOESY cross-peak patterns for Δ17-SG (Figure 5B) and R106T (Figure 5C) were somewhat similar to that for the wild-type protein (Figure 5A); for example, all three exhibited correlations with

[3] Unlike the wild-type and R106T variants of I-FABP, Δ17-SG exhibited a reversible dissociation of ligand with decreasing pH and the fatty acid carboxyl resonance was undetectable at pH values below 5.8.

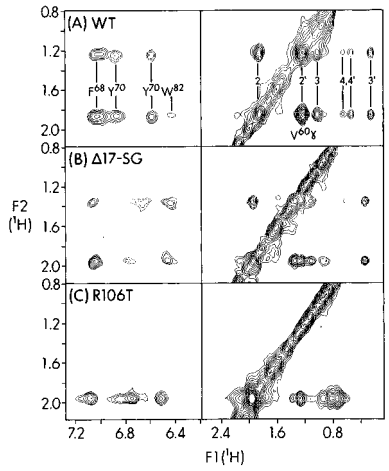


FIGURE 5: Two-dimensional $^1$H/$^{13}$C NOESY−HSQC spectra for [2-$^{13}$C]palmitate bound to wild-type (A), Δ17-SG (B), and R106T (C) I-FABP at 25 °C. Along the *y*-axis, the cross-peak positions represent the H2 and H2′ protons of the bound fatty acid (see the *x*-axis of Figure 3). Along the *x*-axis, the cross-peak positions represent protein and fatty acid protons that are within ~5 Å of the fatty acid H2/H2′. The labels in panel A are derived from the data base of sequence-specific assignments for the wild-type protein (Hodsdon *et al.*, 1995; footnote 2). The protein samples were identical to those in Figure 3: number of transients, 80 (A and B) and 64 (C); number of increments, 350 (A) and 320 (B and C) zero-filled to 1024; spectral widths, 6500 Hz; F2 complex points, 1024 zero-filled to 2048; and mixing time, 220 ms.

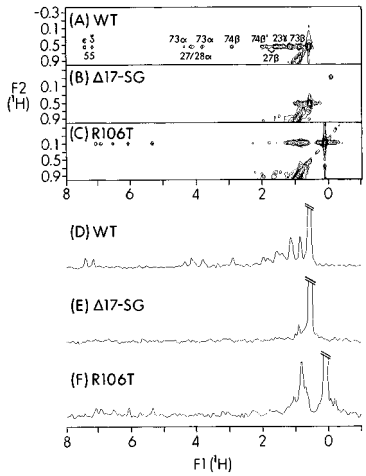


FIGURE 6: Two-dimensional $^1$H/$^{13}$C NOESY−HSQC spectra for [16-$^{13}$C]palmitate bound to wild-type (A and D), Δ17-SG (B and E), and R106T (C and F) I-FABP at 25 °C. For panels A−C, the cross-peak *y*-axis positions represent the methyl protons of the bound fatty acid. Along the *x*-axis, the cross-peak positions represent other protein and fatty acid protons that are within ~5 Å of the fatty acid methyl protons. Panels D−F are F1 traces taken through the most intense part of the fatty acid methyl resonances. The labels in panel A are derived from the data base of sequence-specific assignments for the wild-type protein (Hodsdon *et al.*, 1995; footnote 2): number of transients, 80 (A and C) and 64 (C); number of increments, 330 (A), 320 (B), and 325 (C) zero-filled to 1024; spectral widths, 6500 Hz; F2 complex points, 1024 zero-filled to 2048; and mixing time, 220 ms.

aromatic ring protons consistent with a buried location for the carboxyl end of the fatty acid.

To probe the interactions between the methyl terminus of the fatty acid and the protein, HSQC and NOESY-HSQC (Figure 6) spectra were collected for the [16-$^{13}$C]palmitate−protein complex. In the X-ray and NMR structures of the wild-type protein, the methyl terminus of the fatty acid interacts directly with residues in the α-helical region of the

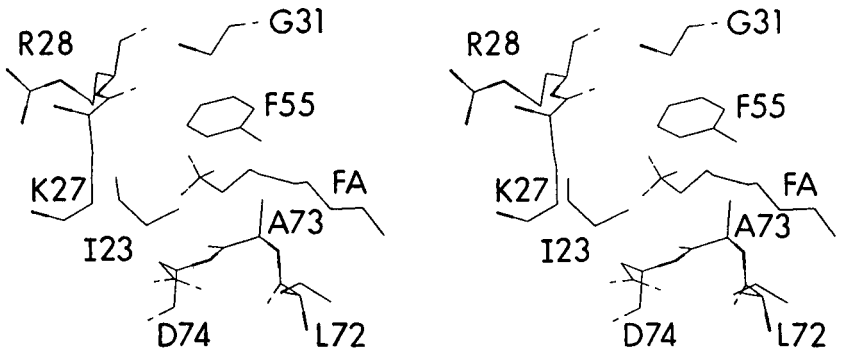


FIGURE 7: Stereodiagram of the region of the I-FABP binding cavity adjacent to the methyl group of palmitate, based on the 2.0 Å crystal structure (Sacchettini *et al.*, 1989). For clarity, only the carbons at positions 9−16 and the protons at position 16 of palmitate are shown. For the protein, the backbone and side chain atoms (except protons) are shown for residues 27, 28, 31, and 72−74. Only the side chain carbons are shown for residues 23 and 55.

protein (Figure 7), and the helices form a cap over that end of the binding cavity. The NMR spectrum for the wild-type protein exhibited cross-peaks between the fatty acid methyl protons and protons from I23, K27, and R28 from the second α-helix (Figure 6A,D). Additional correlations were observed between the fatty acid methyl group and F55, A73, and D74. Fatty acid−protein correlations involving the methyl terminus were also observed for R106T (Figure 6C,F). In striking contrast, few (if any) correlations were observed for Δ17-SG (Figure 6B,E). This result was indicative of a relative absence of contacts between the methyl terminus of the bound fatty acid and Δ17-SG.

*Ligand Binding Kinetics*. Stopped-flow fluorescence experiments were used to measure the association rate constants for oleate binding, and the results are displayed in Figure 8. For both Δ17-SG and wild-type I-FABP, the observed rate constant increased with increasing oleate concentration, as expected for an association process (Figure 8A). However, the rates for the wild-type protein plateaued at ~1000 $s^{-1}$, while those for Δ17-SG continued to increase and became too rapid to quantitate at higher oleate concentrations. As shown in Figure 8B, there was a marked difference in the observed rates for both proteins determined under identical conditions; the binding process was much faster for Δ17-SG. Indeed, binding to Δ17-SG was nearly complete within the dead time of the instrument. Although lowering the I-FABP concentration slowed the rate, the signal was too small to detect, and it was not possible to determine rate constants at lower concentrations. Thus, this experiment provided a minimum value for the association rate constant. Assuming a simple binding mechanism, the observed association rate constant was at least $8 \times 10^7$ $M^{-1}$ $s^{-1}$. Further analysis and interpretation of the kinetic results are provided below.

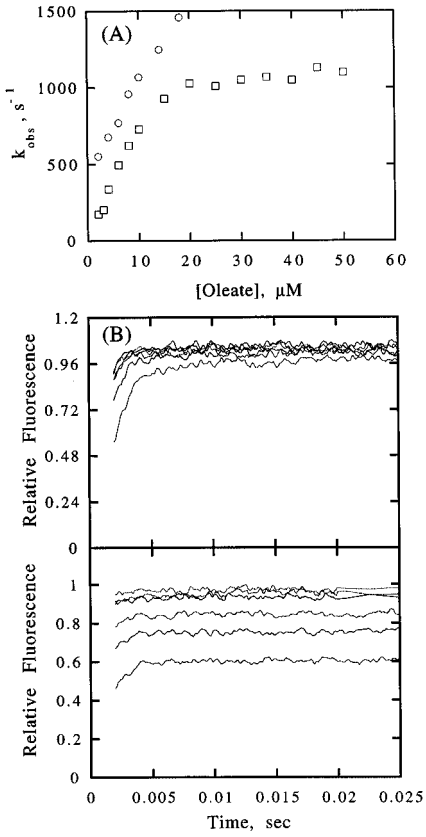


FIGURE 8: (A) Observed association rates for oleate binding to Δ17-SG (circles) and wild-type (squares) I-FABP as a function of ligand concentration as determined from stopped-flow fluorescence experiments. Aliquots of the wild-type (1.0 μM) or Δ17-SG (2.0 μM) proteins were mixed with an equal volume of oleate solutions (4−100 μM). The $k_{obs}$ was estimated from a fit to the first-order rate equation. (B) Stopped-flow traces showing fluorescence changes upon oleate binding to wild-type (upper panel) and Δ17-SG (lower panel) I-FABP. The data for both proteins were collected at the same oleate concentrations (6, 10, 15, 30, 40, and 50 μM) and were normalized to the maximum change observed.

## DISCUSSION

The deletion of a 17-residue segment of I-FABP corresponding to residues 15−31, combined with the insertion of a two-residue linker, resulted in an essentially helix-less, all-β-sheet variant of I-FABP that is remarkably stable and that retains its ability to bind fatty acids. Since no other mutant or wild-type members of the intracellular lipid-binding protein family exhibit a structure lacking α-helices, the Δ17-SG variant of I-FABP provided a unique model system for assessing the role of the α-helical region in the mechanism of ligand binding. The fluorescence and NMR results for Δ17-SG were compared and contrasted with those for wild-type I-FABP and the single-site mutant R106T, and these results provided insights into the nature of fatty acid interactions with the wild-type and mutant proteins.

Three lines of evidence support the conclusion that the carboxyl end of the fatty acid binds to Δ17-SG in a manner similar to that for wild-type I-FABP and forms an ion pair/hydrogen bond network with the protein. First, the HSQC results for [2-$^{13}$C]palmitate bound to Δ17-SG exhibited the characteristic spectral signature observed for wild-type I-FABP. This signature arises from the immobilization of

the carboxyl end of the bound fatty acid by the hydrogen bond network involving Arg106. Second, the ionization behavior of the carboxyl group of fatty acid bound to Δ17-SG was similar to that for the wild-type protein. Both complexes exhibited little ionization and apparently low fatty acid p$K_a$ values, consistent with the formation of fatty acid−protein ion pair interactions. Third, the NOESY cross-peak patterns for the 2-methylene protons of palmitate bound to Δ17-SG were similar to those for wild-type I-FABP. Spectra for both proteins exhibited through-space correlations with aromatic ring protons, consistent with a buried location for the carboxyl end of the bound fatty acid.

In contrast, the interactions between the methyl end of the fatty acid and the protein were distinctly different for Δ17-SG as compared with those for wild-type I-FABP and R106T. For the wild-type protein, nearest neighbor interactions were clearly observed between the fatty acid methyl protons and residues from the helical region as well as the adjacent ends of $\beta$-strands C−D and E−F. In contrast, few or no nearest neighbor interactions were observed between the fatty acid methyl protons and Δ17-SG. This selective lack of NOE cross-peaks involving the methyl end of the fatty acid, combined with the observation of wild-type-like interactions at the carboxyl end, provided further evidence that Δ17-SG contains an essentially intact $\beta$-clam structure, except for the lack of the helical cap covering the methyl end of the binding cavity (Kim *et al.*, 1996). Thus, the α-helices of I-FABP are not required to maintain the overall integrity of the binding cavity.

Removal of the helices increased the dissociation constant by about 20−100-fold and changed the kinetics of binding. The plateau of the observed rates at high oleate concentrations for the wild-type protein (Figure 8A) suggested the presence of a rate-limiting step in the association process. This step could represent some type of conformational change that allows the ligand access to the internal cavity of the wild-type protein. The simplest mechanism to describe the data is

Scheme 1

$$P' \underset{k_{-1}}{\overset{k_1}{\rightleftharpoons}} P$$

$$P + L \underset{k_{-2}}{\overset{k_2}{\rightleftharpoons}} PL$$

where P′ and P denote "closed" and "open" forms of apo-I-FABP, respectively, and L denotes the fatty acid ligand. This mechanism assumes that the P′ form effectively does not bind ligand until it isomerizes and does not differentiate the ligand binding event from any conformational changes that may occur after binding. Since the rate of oleate binding at the plateau is 1000 $s^{-1}$, this value may represent the isomerization rate.

In contrast to those of the wild-type protein, the observed rates of association of oleate with the Δ17-SG did not show a limiting value (Figure 5A) and were indicative of a simple binding mechanism:

Scheme 2

$$P + L \underset{k_{-2}}{\overset{k_2}{\rightleftharpoons}} PL$$

Table 2: Rate Constants Estimated from Kinetic Simulation and Fitting for Oleate Binding to I-FABP

| | $k_1$ ($s^{-1}$) | $k_{-1}$ ($s^{-1}$) | $k_2$ ($\mu M^{-1}$ $s^{-1}$) | $k_{-2}$ ($s^{-1}$) |
|---|---|---|---|---|
| wild-type[a] | 1000 ± 70[b] | 300 ± 130 | 120 ± 10 | 19 ± 1 |
| Δ17-SG[c] | NA[d] | NA | 77 ± 2 | 310 ± 10 |

[a] A mechanism with isomerization followed by ligand binding (Scheme 1)

$$P' \underset{k_{-1}}{\overset{k_1}{\rightleftharpoons}} P; \quad P + L \underset{k_{-2}}{\overset{k_2}{\rightleftharpoons}} PL$$

where P′ and P represent the closed and open form of apo-I-FABP, respectively, and L represents oleate. The best fit was obtained when [P′]:[P] = 2:3. [b] Error estimates are based on a least squares Marquardt fitting of the data using FITSIM (Barshop *et al.*, 1983; Zimmerle & Frieden, 1989). [c] A simple binding mechanism (Scheme 2)

$$P + L \underset{k_{-2}}{\overset{k_2}{\rightleftharpoons}} PL$$

where P denotes the helix-less I-FABP and L denotes oleate. [d] Not applicable.

Thus, there is no apparent kinetic or structural barrier to the acquisition of oleate by the helix-less protein.

The X-ray crystal structure of apo-I-FABP at 1.2 Å revealed no obvious opening that would permit entry of the ligand into the central cavity (Scapin *et al.*, 1992). However, Connally solvent-accessible surface calculations yielded a narrow channel, bounded by α-helix II and turns $\beta$C−$\beta$D and $\beta$E−$\beta$F, that connects the binding cavity with the exterior solvent. The diameter of this channel at its widest point is 5.5 Å, too narrow to accommodate the fatty acid. Thus, some type of conformational change appears to be required for the entry of the fatty acid. The present study provides kinetic evidence for such a conformational change and implies that the helical region may be involved in this change. These results are supported by recent NMR data showing localized disorder in the solution structure of apo-, but not holo-, I-FABP involving a portion of the α-helical domain (M. E. Hodsdon, personal communication). In addition, evidence from limited proteolysis experiments suggests that a similar conformational change may occur in other members of the lipid-binding protein family (Jamison *et al.*, 1994).

The kinetic results also indicated that the association rates for oleate binding to Δ17-SG and wild-type I-FABP were similar, while the dissociation rates for the wild-type protein were 16-fold slower (Table 2). Thus, the α-helical region of I-FABP appears to increase the affinity of I-FABP for fatty acids by selectively lowering the dissociation rate constant.

These results permit speculation regarding possible roles for the α-helical region of I-FABP in the regulation of fatty acid transfer inside the cell. Intracellular FABPs are thought to facilitate the transport of fatty acids across the cytoplasm and their targeting to specific organelles and metabolic pathways. In the cytoplasm, it would be desirable for FABPs to possess a high ligand-binding affinity in order to raise the aqueous solubility of fatty acids and facilitate their flux across the cell. In addition, the high affinity would serve to sequester fatty acids from certain membrane enzymes and ion channels where they may exhibit deleterious effects (Spector, 1986). However, at target sites such as acyl-CoA synthetase in mitochondria, it would be desirable for FABPs to transiently possess a lower affinity for fatty acids in order

to facilitate ligand release. To meet both demands, FABPs may possess a mechanism for regulating their ligand affinity. The results from the present study suggest that the α-helical region could conceivably participate in such a regulatory mechanism.

Transient interactions between FABPs and membrane surfaces have been observed, and these interactions appear to be mediated by ionic interactions between cationic side chains on FABP and anionic groups on membrane lipids (Wootan & Storch, 1994; Herr *et al.*, 1995). It is conceivable that similar interactions between FABP and target sites on organelle surfaces could alter the conformation of the helical region, which in turn might alter the fatty acid dissociation rate and binding affinity. In this way, the release of fatty acids from FABP to target sites on organelles might be facilitated. In the absence of such FABP−membrane interactions, the protein would possess a higher affinity for fatty acids and would be optimized for ligand sequestration and transcytoplasmic diffusion. The helix-less variant of I-FABP provides a model system that could be used in transfer assays and cell culture systems in order to address some of these possibilities.

## ACKNOWLEDGMENT

We thank Katherine Miller for providing the R106T mutant and Michael Hodsdon for helpful discussions.

## REFERENCES

Banaszak, L. B., Winter, N., Xu, Z., Bernlohr, D. A., Cowan, S., & Jones, T. A. (1994) *Adv. Protein Chem. 45*, 89−151.

Barshop, B. A., Wrenn, R. F., & Frieden, C. (1983) *Anal. Biochem. 130*, 134−145.

Bax, A., Ikura, M., Kay, L. E., Torchia, D. A., & Tschudin, R. (1990) *J. Magn. Reson. 86*, 304−318.

Cistola, D. P., & Small, D. M. (1990) *J. Am. Chem. Soc. 112*, 3214−3215.

Cistola, D. P., Atkinson, D., Hamilton, J. A., & Small, D. M. (1986) *Biochemistry 25*, 2804−2812.

Cistola, D. P., Small, D. M., & Hamilton, J. A. (1987) *J. Biol. Chem. 262*, 10980−10985.

Cistola, D. P., Hamilton, J. A., Jackson, D., & Small, D. M. (1988) *Biochemistry 27*, 1881−1888.

Cistola, D. P., Sacchettini, J. C., Banaszak, L. J., Walsh, M. T., & Gordon, J. I. (1989) *J. Biol. Chem. 264*, 2700−2710.

Herr, F. M., Matarese, V., Bernlohr, D. A., & Storch, J. (1995) *Biochemistry 34*, 11840−11845.

Hodsdon, M. E., Toner, J. J., & Cistola, D. P. (1995) *J. Biomol. NMR 6*, 198−210.

Ikura, M., Kay, L. E., Tschudin, R., & Bax, A. (1990) *J. Magn. Reson. 86*, 204−209.

Jakoby, M. G., Miller, K. R., Toner, J. J., Bauman, A., Cheng, L., Li, E., & Cistola, D. P. (1993) *Biochemistry 32*, 872−878.

Jamison, R. S., Newcomer, M. E., & Ong, D. E. (1994) *Biochemistry 33*, 2873−2879.

Kim, K., Cistola, D. P., & Frieden, C. (1996) *Biochemistry 35*, 7553−7558.

Miller, K. R., & Cistola, D. P. (1993) *Mol. Cell. Biochem. 123*, 29−37.

Richieri, G. V., Ogata, R. T., & Kleinfeld, A. M. (1992) *J. Biol. Chem. 267*, 23495−23501.

Richieri, G. V., Ogata, R. T., & Kleinfeld, A. M. (1994) *J. Biol. Chem. 269*, 23918−23930.

Sacchettini, J. C., & Gordon, J. I. (1993) *J. Biol. Chem. 268*, 18399−18402.

Sacchettini, J. C., Gordon, J. I., & Banaszak, L. J. (1989) *J. Mol. Biol. 208*, 327−339.

Scapin, G., Gordon, J. I., & Sacchettini, J. C. (1992) *J. Biol. Chem. 267*, 4253−4269.

Shaka, A. J., Barker, P. B., & Freeman, R. (1985) *J. Magn. Reson. 64*, 547−552.

Spector, A. A. (1986) in *Biochemistry and Biology of Plasma Lipoproteins* (Scanu, A. M., & Spector, A. A., Eds.) pp 247−279, Marcel Dekker, Inc., New York.

Tonomura, B., Nakatani, H., Ohnishi, M., Yamaguchi-Ito, J., & Hiromi, K. (1978) *Anal. Biochem. 84*, 370−383.

Veerkamp, J. H., & Maatman, R. G. H. J. (1995) *Prog. Lipid Res. 34*, 17−52.

Wiseman, T., Williston, S., Brandts, J. F., & Lin, L.-N. (1989) *Anal. Biochem. 179*, 131−137.

Wootan, M. G., & Storch, J. (1994) *J. Biol. Chem. 269*, 10517−10523.

Zimmerle, C. T., & Frieden, C. (1989) *Biochem. J. 258*, 381−387.

BI952912X